Experimental Animals
Exp. Anim. 72(1), 88–94, 2023

Original

The rat Downunder (*Du*) coat color mutation is associated with eye anomalies and embryonic lethality and maps to a 3.9-Mb region on chromosome 3

Hoang Trung HIEU[1)], Miyuu TANAKA[2)], Mitsuru KUWAMURA[2)], Tomoji MASHIMO[3,4)], Tadao SERIKAWA[3,5)] and Takashi KURAMOTO[1,3)]

[1)]*Department of Animal Science, Faculty of Agriculture, Tokyo University of Agriculture, 1737 Funako, Atsugi, Kanagawa 243-0034, Japan*
[2)]*Laboratory of Veterinary Pathology, Graduate School of Veterinary Science, Osaka Metropolitan University, 1-58 Rinku-ourai-kita, Izumisano, Osaka 598-8531, Japan*
[3)]*Institute of Laboratory Animals, Graduate School of Medicine, Kyoto University, Yoshidakonoe-cho, Sakyo-ku, Kyoto 606-8501, Japan*
[4)]*Division of Animal Genetics, The Institute of Medical Science, The University of Tokyo, 4-6-1 Shirokanedai, Minato-ku, Tokyo 108-8639, Japan*
[5)]*Kyoto Disease Model Institute, The Kyoto Technoscience Center, 14 Yoshida-kawara-cho, Sakyo-ku, Kyoto 606-8305, Japan*

Abstract: Rodent coat color genes have been studied as a bioresource to understand developmental and cellular processes. The Downunder rat is a fancy variety with a marking on its belly that runs from the neck to the breech and appears to mirror the dorsal hooded marking. Here, we established a congenic strain carrying the Downunder (*Du*) gene in an F344 genetic background. In addition to the ventral marking, *Du*/+ rats exhibit anophthalmia or microphthalmia with incomplete penetrance. *Du*/*Du* embryos die in the early stages of organogenesis. Genetic linkage analysis mapped the *Du* gene to rat chromosome 3 and haplotype mapping with congenic rats localized the *Du* locus to a 3.9-Mb region. The *Du* locus includes two functional genes, glycosyltransferase-like domain-containing 1 (*Gtdc1*) and zinc finger E-box binding homeobox 2 (*Zeb2*). Although we found no functional variation within any of *Zeb2*'s exons or intron-exon boundaries, *Zeb2* mRNA levels were significantly lower in *Du*/+ rats compared with wild-type rats. It is known that melanocyte-specific *Zeb2* deletion results in the congenital loss of hair pigmentation in mice. Taken together, our results indicate that the *Du* mutation exerts pleiotropic effects on hair pigmentation, eye morphology, and development. Moreover, the *Zeb2* gene is a strong candidate for the *Du* mutation.

Key words: anophthalmia, embryonic lethality, pigmentation, rat, *Zeb2*

Introduction

Rodent mutations that affect either markings or spotting on the coat have contributed to our understanding of melanocyte differentiation and migration [1]. Some coat color mutant strains also serve as models for human diseases. For example, mice carrying the recessive mutation in the endothelin receptor B gene exhibit piebald (white spotting) and megacolon and serve as a model for Waardenburg syndrome type IV [2]. Dominant white spotting mice carry mutations in the *Kit* gene that encodes a receptor tyrosine kinase and serve as a model for piebaldism. Beige mice carry mutations in the *Lyst* gene and serves as a model for Chediak-Higashi syndrome. Thus, identifying genes responsible for coat color pigmentation contributes to greater understanding

(Received 29 June 2022 / Accepted 23 August 2022 / Published online in J-STAGE 19 September 2022)
Corresponding author: T. Kuramoto. email: tk206782@nodai.ac.jp
Supplementary Tables: refer to J-STAGE: https://www.jstage.jst.go.jp/browse/expanim

of physiological processes not only in pigmentation but in signal transduction, membrane trafficking, and development [3].

The Downunder rat is a fancy rat variety with characteristic markings on its belly. The ventral marking is a thick line running from the neck to the breech and is seen only when rats exhibit the hooded phenotype [4]. The Downunder pattern is inherited in a dominant fashion. In 2005, a fancy rat carrying the Downunder (*Du*) mutation was shipped to Japan from a US rat breeder to introduce it into laboratory strains [5]. By crossing this rat with laboratory rats, we generated a congenic strain carrying the *Du* mutation.

For this study, we first established the F344/Cg-*Du* congenic strain and examined eye anomalies in *Du*/+ rats as well as the nature of embryonic lethality among *Du*/*Du* embryos. In addition, we mapped the *Du* mutation to rat chromosome (Chr) 3. By haplotype mapping, we localized the *Du* locus to a 3.9-Mb region that includes two genes, glycosyltransferase-like domain-containing 1 (*Gtdc1*) and zinc finger E-box binding homeobox 2 (*Zeb2*).

Materials and Methods

Animals

A male fancy rat carrying the *Du* mutation was obtained from a rat breeder in Kansas City, MO, USA, in July 2005 [5]. TM/Kyo and WTC/Kyo rats were obtained from the National BioResource Project for the Rat (NBRP-Rat, Kyoto, Japan) [6]. F344/NSlc rats were purchased from Japan SLC, Inc. (Hamamatsu, Shizuoka, Japan). All animal care and experimental procedures used were approved by the Animal Research Committees of Kyoto University and Tokyo University of Agriculture and carried out according to the Regulations on Animal Experimentation of both universities.

Congenic strain

The *Du*-carrying fancy rat was crossed with TM/Kyo rats (coat color genotypes in the *Tyr*$^{+}$ and *H* loci were *C*/*C* and *h*/*h*, respectively), and F1 hybrids were obtained by caesarean section for microbiological cleaning. At the F3 generation, male rats were crossed with WTC/Kyo rats (*c*/*c*, *h*/*h*) to prevent sterility. After three additional inbreeding generations, sperm was collected and cryopreserved.

In 2009, rats carrying the *Du* mutation were rederived by intracytoplasmic sperm injection of F344/NSlc oocytes. Rats carrying the *Du* mutation were identified by the presence of the ventral marking. Because F344/NSlc rats (*c*/*c*, *h*/*h*) were albino, we selected colored Downunder rats and backcrossed them to F344/NSlc rats. After eight generations of backcrossing, we generated the F344.Cg-*Du Tyr*$^{+}$/Kyo congenic strain.

Histopathology

Rats (10–12 weeks of age) were euthanized under isoflurane anesthesia. Brains and eyes were harvested, fixed in 10% neutral buffered formalin, and embedded in paraffin. Four micrometer-thick sections were prepared and stained with hematoxylin and eosin.

Examination of fetuses by cesarean section

Six *Du*/+ female rats were mated with *Du*/+ male rats. At embryonic day 20, fetuses were removed by cesarean section. The numbers of live fetuses and embryo-fetal deaths were counted. Embryo-fetal deaths were classified as either early death (implantation sites, resorbed embryos, and placental remnants) or late death (early macerated fetuses, late macerated fetuses, and dead fetuses). The number of implantations was calculated by summing the number of live fetuses and the number of embryo-fetal deaths.

Genetic mapping

Thirty-nine progeny generated from the (*Du*/+ × WTC)F1 × WTC cross were used for rough mapping. They were genotyped for 25 SSLP markers on Chrs 1, 2, 3, 4, 8, 10, 12, 14, 16, 17, 18, 20, and X (Supplementary Table 1). For fine mapping, 35 F344/NSlc × (F344/NSlc × *Du*/+)F1 backcross progeny were produced. These animals were genotyped for 15 SSLP markers on Chr 3 (Supplementary Table 1).

Next-generation sequencing

A custom capture library was designed with a SureSelect Target Enrichment System (Agilent, Santa Clara, CA, USA). Probes were designed to capture DNA sequences from 24.2 Mb to 28.5 Mb on Chr 3 (USSC rn4, November 2004) that include the genes *Arhgap15*, *Gtdc1*, and *Zeb2*. To construct the library, genomic DNAs from F344.Cg-*Du Tyr*$^{+}$/Kyo (N5) and F344/NSlc were used. A total of 3 μg input DNA per sample was used for SureSelect library preparation (Agilent) with the SureSelect XT HS Target Enrichment System for Illumina Paired-End Multiplexed Sequencing Library (Version 1.6, October 2013) protocol.

Sequencing of SureSelect enriched libraries was performed on an Illumina HiSeq 2500 platform (Illumina, San Diego, CA, USA). Base calling and sample demultiplexing were performed to generate paired FASTQ files for each sample. Adapter sequences were trimmed from raw reads. Reads were discarded when the propor-

tion of bases with a quality score of 10 was less than 95% using FASTX-Toolkit (http://hannonlab.cshl.edu/fastx_toolkit/). Filtered high-quality reads were mapped to the Brown Norway rat strain reference genome (Ensenbl Rat release 69 RGSC 3.4, Dec 2004) using Burrows-Wheeler Alignment tool v0.5.9 [7]. PCR duplicates were removed using Picard v1.93 (http://broadinstitute.github.io/picard). The cleaned alignment files were used to call single nucleotide polymorphisms (SNPs) with Genome Analysis Toolkit v1.6-9 [8], and the effects of variations were annotated using SnpEff v3.5e [9].

Sanger sequencing

Genomic DNA was isolated from the spleen by standard phenol-chloroform extraction and dissolved in TE buffer (10 mM Tris-HCl, pH 8.0, 1 mM EDTA). The exons and intron-exon boundaries of *Gtdc1* and *Zeb2* were amplified with specific primer sets (Supplementary Table 2) and KAPA2G™ Robust HotStart ReadyMix with dye (Merck KGaA, Darmstadt, Germany). Direct sequencing was performed by Macrogen Japan Corp. (Tokyo, Japan).

Quantitative PCR

Total RNA was isolated from rat brains using a FastGene™ RNA Premium Kit (NIPPON Genetics Co., Ltd., Tokyo, Japan). Complementary DNA (cDNA) was synthetized using FastGene™ Scriptase II (NIPPON Genetics Co., Ltd.). Quantitative reverse transcription PCR was performed using a Thermal Cycler Dice Real Time system (Takara Bio Inc., Shiga, Japan) with a KAPA SYBR Fast qPCR Kit (Roche Diagnostics K.K., Tokyo, Japan). The primer sequences for quantifying cDNA were as follows: 5′-ATACCAGCGGAAACAAGGATTTCA-3′ and 5′-CAGGAATCGGAGTCTGTCAAGTCA-3′ for *Zeb2*, and 5′-GTTGTCATCTCAACAGCCAAGCA-3′ and 5′-CAAGTCTTTGGGACAGAGTGGGTAA-3′ for *Gtdc1*. By monitoring the amplification curves of a test sample and reference samples that contained between 10^1 and 10^6 molecules of the mRNA of interest, the number of target mRNA molecules in the test sample was determined and normalized to the amount of glyceraldehyde-3-phosphate dehydrogenase (*Gapdh*) mRNA. The primer sequences of *Gapdh* were as follows: 5′-GGCACAGTCAAGGCTGAGAATG-3′and 5′-ATGGTGGTGAAGACGCCAGTA-3′.

Results

F344.Cg-*Du Tyr*$^+$/Kyo congenic strain

F344.Cg-*Du Tyr*$^+$/Kyo congenic heterozygous rats (*Du*/+) exhibited the characteristic ventral marking, very similar to the original *Du*-carrying rats. The dorsal marking, which was caused by the hooded mutation, of the congenic *Du*/+ rats was wider than that of their wild-type littermates (Fig. 1).

Eye anomalies

Some *Du*/+ rats exhibited eye anomalies that presented as microphthalmia and anophthalmia (Fig. 2A). We examined a total of 70 *Du*/+ rats, of which 16 (22.9%) exhibited such eye anomalies. Of these 16 animals, three had anomalies in their right eye, nine in their left eye, and four had anomalies in both eyes (Fig. 2B). Eye anomalies were observed more frequently in the left eye but this difference was not statistically significant (P=0.083). Anophthalmia was accompanied by loss of the optic nerve (Fig. 2A). Histologically, the anophthalmia showed the complete loss of the eye structures, including lens, cornea, retina, and uvea (Fig. 2C). In severe microphthalmia cases, there was only a small mass of pigmented intraocular remnant/vestigial tissue resembling ciliary processes (Fig. 2C), while the ocular ad-

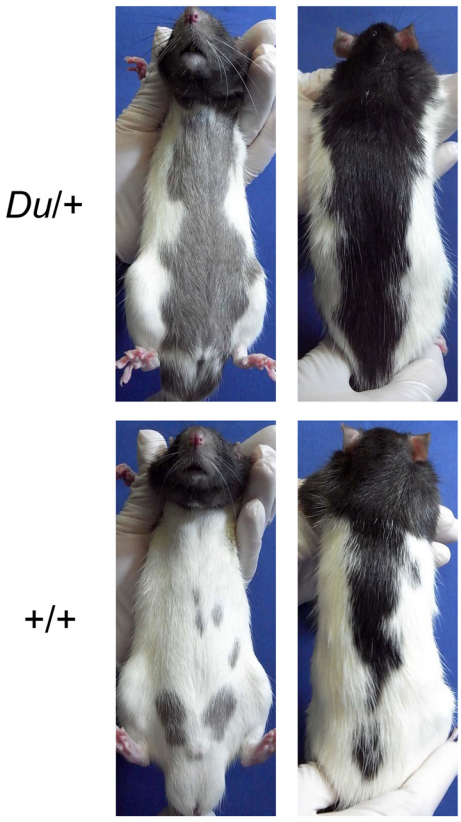

Fig. 1. Ventral and dorsal markings on F344.Cg-*Du Tyr*$^+$/Kyo congenic rats. Top: *Du*/+ heterozygous rat. Bottom: wild-type (+/+) littermate. Ventral markings were prominent on *Du*/+ rats. Dorsal markings were wider than on wild-type rats. Both rats were homozygous for the hooded (*h*) mutation.

 doi: 10.1538/expanim.22-0086

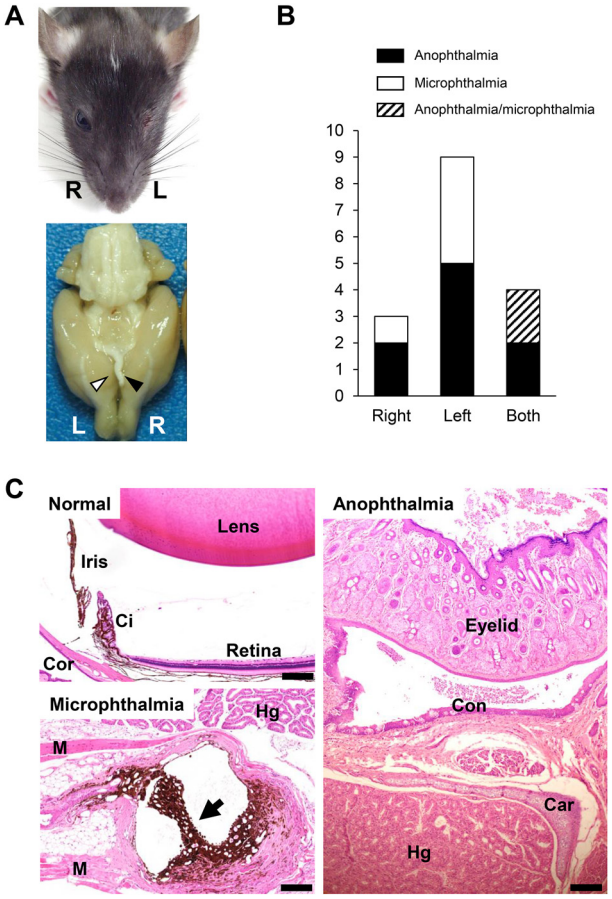

Fig. 2. Eye anomalies in F344.Cg-*Du Tyr*$^{+}$/Kyo congenic rats. A. Upper: Dorsal view of the head of a *Du*/+ rat with an eye anomaly. The left (L) eye is absent. Lower: Ventral view of the brain harvested from the rat in the upper panel. The optic nerve from the right (R) eye is intact (arrowhead), but that from the left (L) eye (white arrowhead) is absent. B. Number of rats exhibiting eye anomalies. Out of 70 rats examined, 16 (22.9%) exhibited eye anomalies. The observed eye anomalies consisted of anophthalmia and microphthalmia. Two *Du*/+ rats exhibited anophthalmia in the right eye and microphthalmia in their left eye; the bar representing these rats contains hatched lines. C. Microscopic images of normal eye, anophthalmia (shown in panel A), and microphthalmia cases. The normal eye consists of an intact lens, retina, ciliary body (Ci), iris, and cornea (Cor). The eye with microphthalmia lacks a lens, cornea, and retina, but a pigmented intraocular vestigial mass (arrow) is present. In the anophthalmia case, these intrinsic structures of the eye are completely absent. The ocular adnexa, including Harderian glands (Hg), eyelid, conjunctiva (Con), and muscle (M), are normal in both microphthalmia and anophthalmia. Car: cartilage. Bars: 200 μm.

nexa, inclufing Harderian glands, lacrimal glands, eyelid, conjunctiva, and extraocular muscles, were almost normal. Such anomalies were not observed in wild-type littermates. These findings indicate that the *Du* mutation also caused the eye anomalies with incomplete penetrance.

Table 1. Number of dead embryos and fetuses observed in *Du*/+ females mated with *Du*/+ males at E20

Stage	Number of fetuses	Mean ± SD
Viable	37	6.2 ± 2.9
Embryonic death (total)	16	2.7 ± 1.9
Implantation site	3	0.5 ± 1.2
Resorbed embryo	12	2.0 ± 1.7
Placental remnant	1	0.2 ± 0.4
Early macerated fetuses	0	0.0 ± 0.0
Late macerated fetuses	0	0.0 ± 0.0
Dead fetuses	0	0.0 ± 0.0

Embryonic lethality

To examine the incidence and stage of embryonic lethality, we crossed *Du*/+ females with *Du*/+ males. We observed 37 live fetuses and 16 embryo-fetal deaths from six pregnant *Du*/+ rats. The proportion of embryo-fetal deaths relative to the number of implantations was 30.2%, compared with 25% embryo-fetal death when homozygous lethality occurred in *Du*/*Du* embryos (P=0.78). Reasons for embryonic deaths included implantation site (0.5 ± 1.2; average ± SD), resorbed embryo (2.0 ± 1.7), and placental remnant (0.2 ± 0.4; Table 1). This finding suggests that *Du*/*Du* embryos died in the early stage of organogenesis (gestation days 10 to 12) [10].

Genetic mapping of *Du* mutation

We observed 21 Downunder (*Du*/+) and 18 non-Downunder (+/+) rats in (*Du*/+ × WTC)F1 × WTC/Kyo backcross progeny (n=39), indicating that *Du* is a single dominant mutation (P=0.63). The initial screening revealed that *Du* was significantly linked with *D3Mgh16* (P<0.001) and *D3Mgh19* (P<0.001). To map *Du* to Chr 3, we further performed a linkage analysis using F344/NSlc × (F344/NSlc × *Du*/+)F1 backcross progeny (n=35) and thereby mapped *Du* to between *D3Rat229* and *D3Rat190*. *Du* showed no recombination with *D3Rat49* (27.5 Mb), *D3Got21* (27.6 Mb), and *D3Got18* (27.9 Mb; Fig. 3A).

To develop SNP markers and identify variations specific to the *Du* allele, we performed next-generation sequencing (NGS) of a 4.21-Mb region within the *Du* locus. The targeted region spans nucleotides 27,944,460 to 32,154,450 of the Chr 3 reference genome (mRatBN7.2). We identified 5,439 variations within the targeted region (Fig. 3B). Representative SNP markers that can be used for haplotype mapping with congenic rats were summarized in Supplementary Table 3. At the N19 generation, a 3.9-Mb region defined by *rs197659597* and *D3Rat190* segregated with the Downunder phenotype, which demonstrated that the *Du* locus lies within this 3.9-Mb region (Fig. 3B). Two genes, *Gtdc1* and *Zeb2*,

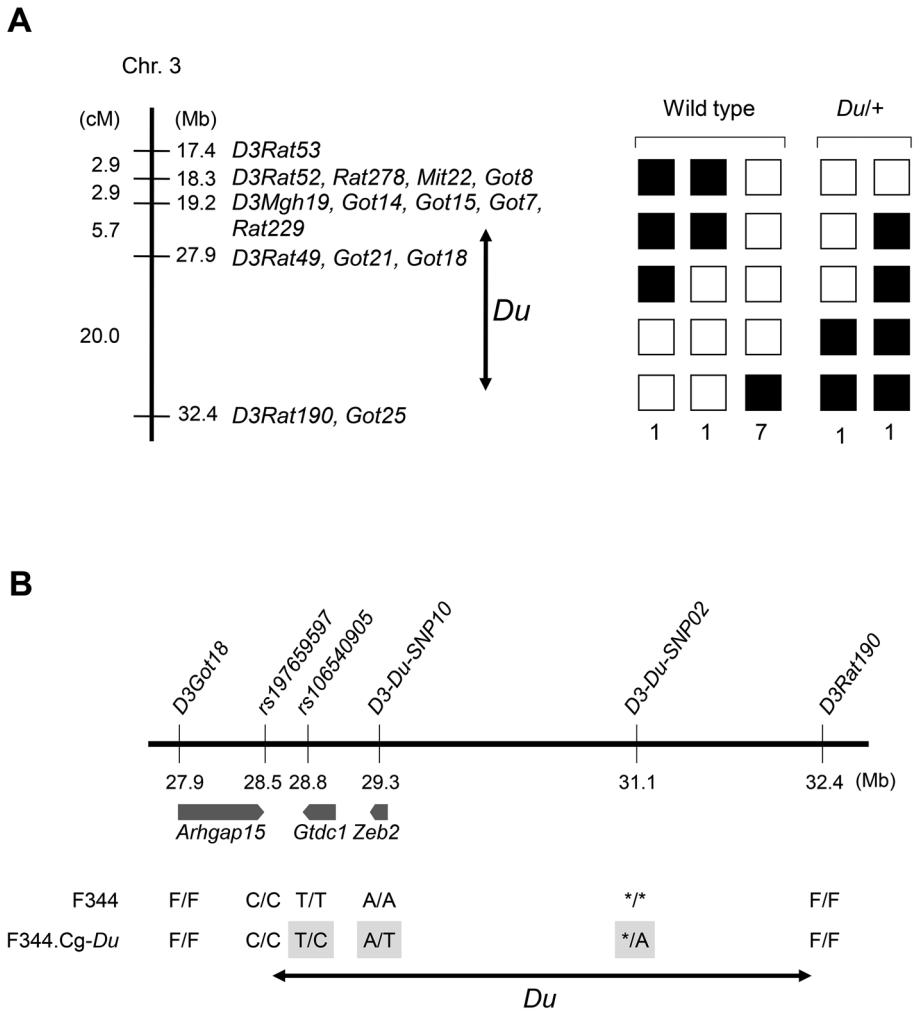

Fig. 3. Genetic mapping of the *Du* locus. A. Left: Genetic linkage map that includes the *Du* locus. Right: Haplotypes observed among backcross progeny carrying the recombinant chromosome between *D3Rat53* and *D3Got25*. Filled boxes represent heterozygous genotypes, whereas open boxes represent homozygous genotypes. The *Du* locus was mapped between *D3Ra229* and *D3Rat190*. B. Physical map of the *Du* locus. Top: Physical positions of genetic markers used to define the *Du* locus and numbers of single nucleotide polymorphisms (SNPs) that were identified by next-generation sequencing (NGS). Bottom: Genotypes of the F344 and F344.Cg-*Du* congenic strains. The F344.Cg-*Du* strain exhibited a heterozygous genotype, highlighted in grey, for the *rs106540905*, *D3-Du-SNP10*, and *D3-Du-SNP02* SNP markers. Genotypes of SNP markers are represented by nucleotides. Asterisks indicate no nucleotide at the *D3-Du-SNP02* SNP marker; the F344 genome has no nucleotides and the *Du* allele has an "A" nucleotide at the SNP. We mapped the *Du* locus to between *rs197659597* and *D3Rat190*, which includes the genes *Gtdc1* and *Zeb2*. F/F: homozygous for the F344 allele in SSLP markers.

were mapped to the *Du* locus. No variation specific to the *Du* allele was found in any of the exons or splice sites of these genes, which was verified by Sanger sequencing.

Gene expression analysis

To find more potential candidate genes, we determined *Gtdc1* and *Zeb2* transcript levels in *Du*/+ rat brains. The relative expression level of *Gtdc1* in *Du*/+ rats did not differ from that of wild-type rats (mean ± SD; $3.93 \times 10^{-2} \pm 3.45 \times 10^{-2}$ vs. $1.42 \times 10^{-2} \pm 0.82 \times 10^{-2}$, P=0.0700). In contrast, *Zeb2* levels were significantly reduced (mean ± SD; $6.35 \times 10^{-2} \pm 1.84 \times 10^{-2}$ vs. $3.19 \times 10^{-2} \pm 2.44 \times 10^{-2}$, P=0.0156; Fig. 4). This finding suggests that *Zeb2* is the likely candidate gene for the *Du* mutation.

Discussion

In this study, we established the F344.Cg-*Du* congenic line, discovered eye anomalies in *Du*/+ rats, determined the developmental stage at which *Du*/*Du* em-

 doi: 10.1538/expanim.22-0086

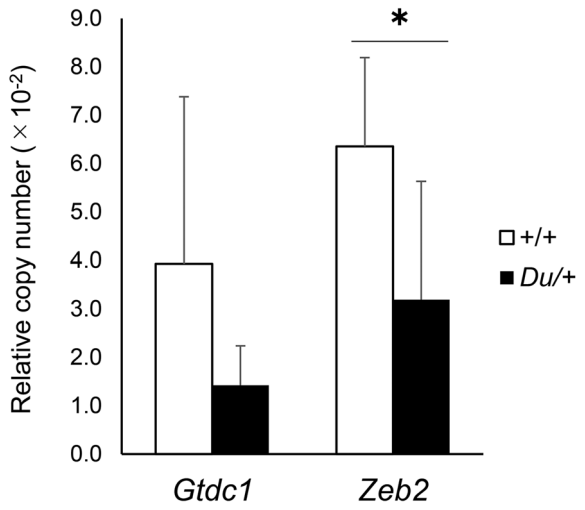

Fig. 4. Relative *Gtdc1* and *Zeb2* mRNA levels in *Du*/+ rats. Relative *Gtdc1* and *Zeb2* mRNA levels in wild-type (open bars) and *Du*/+ (filled bars) rats (n=3, each). *Zeb2* mRNA was significantly reduced in *Du*/+ rat brains compared with wild-type rat brains. **P*<0.02.

bryos die, and localized the *Du* locus to a 3.9-Mb region on rat Chr 3. The *Du* locus includes *Gtdc1* and *Zeb2*. Additionally, we found that *Zeb2* mRNA levels are significantly lower in *Du*/+ rats compared with wild-type rats.

Gtdc1 encodes glycosyltransferase-like domain-containing 1 which was cloned from a fetal brain cDNA library by a high throughput DNA sequencing analysis [11]. Glycosyltransferase catalyzes the synthesis of carbohydrate portions of glycoproteins, glycolipids, and proteoglycans, but GTDC1 function remains unknown. *Gtdc1* transcripts are expressed at relatively high levels in the adult lung, spleen, testis, and peripheral blood leukocytes [11]. The *GTDC1* gene was reportedly disrupted in a human patient with signs of neurodevelopmental disorders, while *gtdc1* knockdown in zebrafish led to impaired CNS development [12]. *Gtdc1*-modified mice have not been developed, and no information on *Gtdc1* involvement in pigmentation is currently available.

Zeb2 encodes a transcription factor called zinc finger E-box binding homeobox 2. In humans, mutations in the *ZEB2* gene are known to cause Mowat-Wilson Syndrome (MOWS; OMIM #235730), an autosomal dominant complex disorder [13, 14]. MOWS patients exhibit typical facial dimorphism but suffer from severe intellectual disability and delayed motor development. Additionally, anomalies are often observed in the corpus callosum or the hippocampus, if not both. Other anomalies have been observed in the urogenital tract, eye, ear, and heart. MOWS patients also often suffer from Hirschsprung disease (HSCR), which affects the gastrointestinal tract [15–17].

Homozygous *Zeb2*-knockout (KO) mice are embryonic lethal; they are severely retarded in their growth by E9.5 before dying [18]. Heterozygous *Zeb2*-KO mice exhibit craniofacial abnormalities and corpus callosum formation defect but not abnormal pigmentation [19]. Moreover, melanocyte-specific *Zeb2* deletion resulted in the congenital loss of hair pigmentation in mice, which suggests an essential role for *Zeb2* in pigmentation [20]. Additionally, we detected a significantly lower level of *Zeb2* transcripts in *Du*/+ rats. Taken together, these observations suggest that *Zeb2* is a strong candidate gene for the *Du* mutation.

We did not find any variations specific to the *Du* allele in any of the exons or intron-exon boundaries of *Zeb2*, which suggests that the causative variation may be found in a regulatory region (usually located upstream of a gene) of *Zeb2*. The *Du* locus includes at least a 3.0-Mb upstream region of *Zeb2*, and we identified an ample number of variations in the *Du* locus by NGS. In a follow-up study, we will sort through these variations using bioinformatics analyses that can predict enhancers and regulatory regions. Alternatively, the causative variation may be an insertion of DNA such as transposable elements. To find such variations, sequencing of large DNA fragments derived from the *Du* locus is necessary, and may be accomplished by either constructing a BAC library [21] or nanopore DNA sequencing [22].

The ventral marking of *Du*/+ rats closely resembles to the marking of black-and-tan (a^t/a^t) mice in which a sharp dorso-ventral boundary is observed [23]. Formation of the boundary in a^t/a^t mice is modified by *Tbx15* [24]. These findings suggest that the pigmentation of the ventral coat differs from that of the dorsal coat and that the pigmentation area is regulated by genetic factors. Thus, we speculate that the downunder marking may result from the visualization of the ventral-specific pigmentation in rats and that the *Du* mutation, possibly the *Zeb2* downregulation, may interact with genes involved in the formation of the dorso-ventral boundary.

Lastly, we found that the *Du* mutation usually manifests phenotypically in hooded (*h*/*h*) rats that exhibit white markings on their ventral and lateral trunk. The hooded phenotype is unique to rats and is prevalent among most rat strains [25], which enabled us to follow the *Du* mutation. Thus, the availability of different species of model animals is crucial to identifying novel gene functions.

In summary, in addition to ventral markings, the *Du* mutation is associated with eye anomalies and early postgestation lethality. The *Du* locus is located within a 3.9-Mb genomic region on Chr 3, and *Zeb2* is the most likely candidate gene.

Acknowledgments

We are grateful to Dr. H. Hiai for useful comments on the eye anomalies and M. Yokoe for technical assistance. We also thank the NBRP-Rat in Japan for providing the TM/Kyo (NBRP Rat No: 0014) and WTC/Kyo (NBRP Rat No: 0020) rat strains and for preserving the congenic strain F344.Cg-*Du Tyr*$^{+}$/Kyo (NBRP Rat No: 0669) congenic strain. This study was supported in part by JSPS KAKENHI Grant Number 25640046.

References

1. Jackson IJ. Homologous pigmentation mutations in human, mouse and other model organisms. Hum Mol Genet. 1997; 6: 1613–1624. [Medline] [CrossRef]
2. Matsushima Y, Shinkai Y, Kobayashi Y, Sakamoto M, Kunieda T, Tachibana M. A mouse model of Waardenburg syndrome type 4 with a new spontaneous mutation of the endothelin-B receptor gene. Mamm Genome. 2002; 13: 30–35. [Medline] [CrossRef]
3. Bennett DC, Lamoreux ML. The color loci of mice--a genetic century. Pigment Cell Res. 2003; 16: 333–344. [Medline] [CrossRef]
4. Perez C. Unique dominant rat spotting gene known as australian downunder − may represent a new major spotting gene of rattus norvegicus. Pigment Cell Res. 2004; 17: 451. [CrossRef]
5. Kuramoto T, Yokoe M, Yagasaki K, Kawaguchi T, Kumafuji K, Serikawa T. Genetic analyses of fancy rat-derived mutations. Exp Anim. 2010; 59: 147–155. [Medline] [CrossRef]
6. Serikawa T, Mashimo T, Takizawa A, Okajima R, Maedomari N, Kumafuji K, et al. National BioResource Project-Rat and related activities. Exp Anim. 2009; 58: 333–341. [Medline] [CrossRef]
7. Li H, Durbin R. Fast and accurate short read alignment with Burrows-Wheeler transform. Bioinformatics. 2009; 25: 1754–1760. [Medline] [CrossRef]
8. McKenna A, Hanna M, Banks E, Sivachenko A, Cibulskis K, Kernytsky A, et al. The Genome Analysis Toolkit: a MapReduce framework for analyzing next-generation DNA sequencing data. Genome Res. 2010; 20: 1297–1303. [Medline] [CrossRef]
9. Cingolani P, Platts A, Wang L, Coon M, Nguyen T, Wang L, et al. A program for annotating and predicting the effects of single nucleotide polymorphisms, SnpEff: SNPs in the genome of Drosophila melanogaster strain w1118; iso-2; iso-3. Fly (Austin). 2012; 6: 80–92. [Medline] [CrossRef]
10. Erb C. Embryology and teratology. In: Suckow MA, Weisbroth SH, Franklin CL, editors. The laboratory rat. Burlington, MA: Elsevier Academic Press; 2006. pp. 817–846.
11. Zhao E, Li Y, Fu X, Zhang JY, Zeng H, Zeng L, et al. Cloning and expression of human GTDC1 gene (glycosyltransferase-like domain containing 1) from human fetal library. DNA Cell Biol. 2004; 23: 183–187. [Medline] [CrossRef]
12. Aksoy I, Utami KH, Winata CL, Hillmer AM, Rouam SL, Briault S, et al. Personalized genome sequencing coupled with iPSC technology identifies *GTDC1* as a gene involved in neurodevelopmental disorders. Hum Mol Genet. 2017; 26: 367–382. [Medline] [CrossRef]
13. Cerruti Mainardi P, Pastore G, Zweier C, Rauch A. Mowat-Wilson syndrome and mutation in the zinc finger homeo box 1B gene: a well defined clinical entity. J Med Genet. 2004; 41: e16. [Medline] [CrossRef]
14. Wakamatsu N, Yamada Y, Yamada K, Ono T, Nomura N, Taniguchi H, et al. Mutations in *SIP1*, encoding Smad interacting protein-1, cause a form of Hirschsprung disease. Nat Genet. 2001; 27: 369–370. [Medline] [CrossRef]
15. Zweier C, Albrecht B, Mitulla B, Behrens R, Beese M, Gillessen-Kaesbach G, et al. "Mowat-Wilson" syndrome with and without Hirschsprung disease is a distinct, recognizable multiple congenital anomalies-mental retardation syndrome caused by mutations in the zinc finger homeo box 1B gene. Am J Med Genet. 2002; 108: 177–181. [Medline] [CrossRef]
16. Garavelli L, Zollino M, Mainardi PC, Gurrieri F, Rivieri F, Soli F, et al. Mowat-Wilson syndrome: facial phenotype changing with age: study of 19 Italian patients and review of the literature. Am J Med Genet A. 2009; 149A: 417–426. [Medline] [CrossRef]
17. Garavelli L, Donadio A, Zanacca C, Banchini G, Della Giustina E, Bertani G, et al. Hirschsprung disease, mental retardation, characteristic facial features, and mutation in the gene *ZFHX1B* (*SIP1*): confirmation of the Mowat-Wilson syndrome. Am J Med Genet A. 2003; 116A: 385–388. [Medline] [CrossRef]
18. Van de Putte T, Maruhashi M, Francis A, Nelles L, Kondoh H, Huylebroeck D, et al. Mice lacking *ZFHX1B*, the gene that codes for Smad-interacting protein-1, reveal a role for multiple neural crest cell defects in the etiology of Hirschsprung disease-mental retardation syndrome. Am J Hum Genet. 2003; 72: 465–470. [Medline] [CrossRef]
19. Takagi T, Nishizaki Y, Matsui F, Wakamatsu N, Higashi Y. De novo inbred heterozygous *Zeb2*/*Sip1* mutant mice uniquely generated by germ-line conditional knockout exhibit craniofacial, callosal and behavioral defects associated with Mowat-Wilson syndrome. Hum Mol Genet. 2015; 24: 6390–6402. [Medline] [CrossRef]
20. Denecker G, Vandamme N, Akay O, Koludrovic D, Taminau J, Lemeire K, et al. Identification of a ZEB2-MITF-ZEB1 transcriptional network that controls melanogenesis and melanoma progression. Cell Death Differ. 2014; 21: 1250–1261. [Medline] [CrossRef]
21. Kuramoto T, Voigt B, Nakanishi S, Kitada K, Nakamura T, Wakamatsu K, et al. Identification of candidate genes for generalized tonic-clonic seizures in Noda Epileptic Rat. Behav Genet. 2017; 47: 609–619. [Medline] [CrossRef]
22. Miller DE, Sulovari A, Wang T, Loucks H, Hoekzema K, Munson KM, et al. University of Washington Center for Mendelian Genomics. Targeted long-read sequencing identifies missing disease-causing variation. Am J Hum Genet. 2021; 108: 1436–1449. [Medline] [CrossRef]
23. Bultman SJ, Klebig ML, Michaud EJ, Sweet HO, Davisson MT, Woychik RP. Molecular analysis of reverse mutations from nonagouti (*a*) to black-and-tan (a^{t}) and white-bellied agouti (A^{w}) reveals alternative forms of agouti transcripts. Genes Dev. 1994; 8: 481–490. [Medline] [CrossRef]
24. Candille SI, Van Raamsdonk CD, Chen C, Kuijper S, Chen-Tsai Y, Russ A, et al. Dorsoventral patterning of the mouse coat by *Tbx15*. PLoS Biol. 2004; 2: E3. [Medline] [CrossRef]
25. Kuramoto T, Nakanishi S, Ochiai M, Nakagama H, Voigt B, Serikawa T. Origins of albino and hooded rats: implications from molecular genetic analysis across modern laboratory rat strains. PLoS One. 2012; 7: e43059. [Medline] [CrossRef]